

# ULRR

## A facile spin-cast route for cation exchange of multilayer perpendicularly-aligned nanorod assemblies

Item Type	Article
Authors	Kelly, Dervla;Singh, Ajay;Barrett, Christopher A.;O'Sullivan, Catriona;Coughlan, Claudia;Laffir, Fathima R.;O'Dwyer, Colm;Ryan, Kevin M.
Citation	Nanoscale;3, pp. 4580-4583
Publisher	Royal Society of Chemistry
Download date	2026-06-17 16:45:33
Item License	<a href="https://creativecommons.org/licenses/by-nc-sa/1.0/">https://creativecommons.org/licenses/by-nc-sa/1.0/</a>
Link to Item	<a href="https://hdl.handle.net/10344/2555">https://hdl.handle.net/10344/2555</a>

Cite this: DOI: 10.1039/c0xx00000x

www.rsc.org/xxxxxx

ARTICLE TYPE

# A Facile Spin-Cast Route for Cation Exchange of Multilayer Perpendicularly-Aligned Nanorod Assemblies†

Dervla Kelly,<sup>a,b,c</sup> Ajay Singh<sup>abc</sup>, Christopher A. Barrett<sup>ab,†</sup>, Catriona O'Sullivan<sup>ab</sup>, Claudia Coughlan<sup>ab</sup>, Fathima R. Laffir<sup>a</sup>, Colm O'Dwyer<sup>ad</sup> and Kevin M. Ryan<sup>\*abc</sup>

5 Received (in XXX, XXX) Xth XXXXXXXXXX 20XX, Accepted Xth XXXXXXXXXX 20XX

DOI: 10.1039/b000000x

A facile spin cast route was developed to convert perpendicularly aligned nanorod assemblies of cadmium chalcogenides into their silver and copper analogues. The assemblies are rapidly cation exchanged without affecting either the individual rod dimensions or collective superlattice order extending over several multilayers.

Semiconductor nanorod assembly offers a viable route to integrating non-equilibrium shaped nanorods into high density applications, such as solar cells<sup>1</sup>. Vertical alignment of nanorods allows the material properties such as linear polarised emission and total photon absorption to be easily harnessed into scalable applications.<sup>2</sup> External directing agents such as the use of highly oriented pyrolytic graphite<sup>3</sup>, electrophoresis and electric field assisted assembly<sup>4</sup> have all proven successful in large scale assembly formation. Parallel to these techniques, there are a variety of successful self assembly techniques including controlled drying techniques<sup>5</sup>, depletion attraction<sup>6</sup> and kinetically driven approaches<sup>7</sup>. All methods are critically dependent upon low polydispersity in both nanorod length and diameter to achieve assembly. While colloidal routes to cadmium chalcogenides are well studied, giving accurate dimensional control in high yield, similar successes with copper and silver chalcogenides have remained elusive.<sup>8</sup> Assemblies of these materials, in nanorod form, are of particular interest in photovoltaics where their wide-band gap absorption coupled with high material abundance and low toxicity make them an attractive long-term PV solution<sup>9</sup>.

Cation exchange is a facile method for conversion of II-VI semiconductor nanorods into their I-VI analogues by replacing cadmium with either silver or copper<sup>10</sup>. The chemical transformation of the nanocrystalline solid occurs via diffusion or exchange of atoms that is only kinetically feasible at the nanoscale.<sup>11</sup> Once the rods are above a critical size threshold, the nanorod structure remains intact, conserving the same shape and monodispersity of the original CdS or CdSe nanorods.<sup>12</sup> The cation exchange route therefore allows a range of silver and copper containing nanorods to be formed in high yield with controlled dimensions, which otherwise would not be readily attainable by synthetic approaches. Recycling the cadmium from solution for subsequent syntheses has been demonstrated allowing for its sacrificial use for high throughput production of copper and silver materials with minimal environmental impact.<sup>13</sup>

Here, we demonstrate the multilayer assembly of CdS and CdSe nanorods over large areas and their subsequent conversion to copper and silver chalcogenides by a facile spin exchange procedure. By adopting this approach, we were able to maintain the structure of the existing assemblies while altering the composition. Although partial exchange within each rod in a monolayer assembly (CdS to Cu<sub>2</sub>S) has been shown,<sup>14</sup> our instantaneous conversion of up to 30 multilayers is optimal for total absorption of incident light (PV) at device scales of micron thicknesses and square centimetre areas. In addition, this spin cast approach is generally applicable and is extended to the formation of multilayer assemblies of Ag<sub>2</sub>S, Ag<sub>2</sub>Se, Cu<sub>7</sub>S<sub>4</sub>, and Cu<sub>3</sub>Se<sub>2</sub> from the respective cadmium chalcogenides while retaining vertical alignment and close packed order.

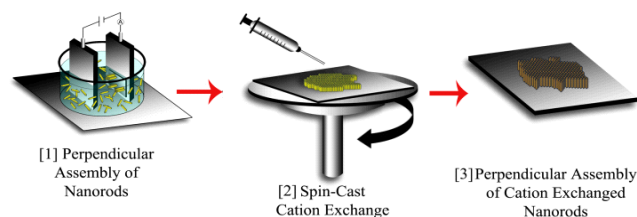


**Fig.1** Schematic of spin exchange process showing; [1] Alignment of nanorods by electrophoretic deposition, [2] Spin-cast exchange and [3] The final cation exchanged assembly.

The schematic shown in Fig. 1 illustrates the spin exchange process where assembled cadmium chalcogenide rods are completely converted into their copper or silver analogues by the introduction of a solution of the desired cation dissolved in methanol. (More detailed experimental data in supplementary information.) The centrifugal forces generated during spin casting allows for the conformal distribution of the solution throughout the layer of nanorods for uniform exchange. The subsequent spin-casting of methanol (hard Lewis base) binds effectively to the Cd<sup>2+</sup> ions (hard Lewis acid) making exchange energetically favourable, even on the short solvent dwell times of the spin-cast process<sup>15</sup>. To demonstrate the feasibility of the exchange a dilute dispersion of non-aligned rods was prepared. Fig. 2 (a) shows a HRTEM image of unaligned cadmium sulphide nanorods with corresponding electron diffraction pattern indexed showing rings which are consistent with the [0,1,0], [0,1,2], [0,2,0] and [1,1,2] reflections for wurtzite CdS. Fig. 2(b) shows the converted Cu<sub>7</sub>S<sub>4</sub> demonstrating the conservation of both size and shape

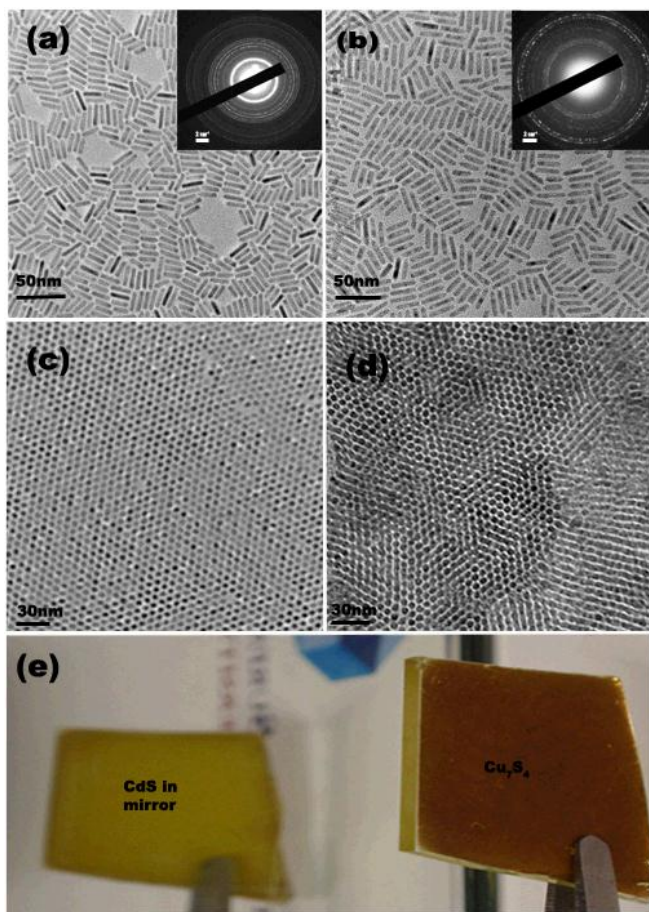


**Fig.2** (a) HRTEM of non aligned CdS nanorods and inset electron diffraction (b) HRTEM of non aligned  $\text{Cu}_7\text{S}_4$  nanorods with inset of electron diffraction pattern (c) HRTEM of vertically aligned CdS nanorods (d) HRTEM of aligned  $\text{Cu}_7\text{S}_4$  nanorods and (e) Assembly partially exchanged using spin exchange process, the CdS can be seen in the mirror and the  $\text{Cu}_7\text{S}_4$  can be seen in the foreground.

distribution. The corresponding electron diffraction shows rings indexed to the [1,0,3], [1,1,3], [3,0,1] and [0,0,2] reflections corresponding to crystalline  $\text{Cu}_7\text{S}_4$ . (Larger images of electron diffraction can be seen in Supplementary Information Fig. S1 & Fig. S2 (ESI<sup>†</sup>)) The copper deficiency is typical in copper chalcogenides where multiple stoichiometric variations of copper sulphide exist. The initial perpendicular assembly of CdS rods and the exchanged assembly of  $\text{Cu}_7\text{S}_4$  are shown in TEM images in Fig. 2 (c) & (d) respectively. Remarkably, the assemblies remain fully intact after the exchange retaining both the anion sublattice of each discrete rod and the order and packing density of the parent supercrystal. In a centimetre scale multi-layer assembly shown in Fig. 1(e), deposited on ITO on glass, the exchange proceeds from the top-surface with a noticeable colour change from yellow (CdS) to brown ( $\text{Cu}_7\text{S}_4$ ) as the reaction progresses. The retention of the CdS at the ITO side (from mirror image) indicates a layered exchange achieved by controlling the concentration of the cation solution and solvent in contact with the layer. The versatility of this technique for conversion of cadmium sulphide and selenides into both copper and silver chalcogenides is outlined in the XRD study in Fig. 3. Here, large scale assemblies similar to Fig. 1(e) are completely cation

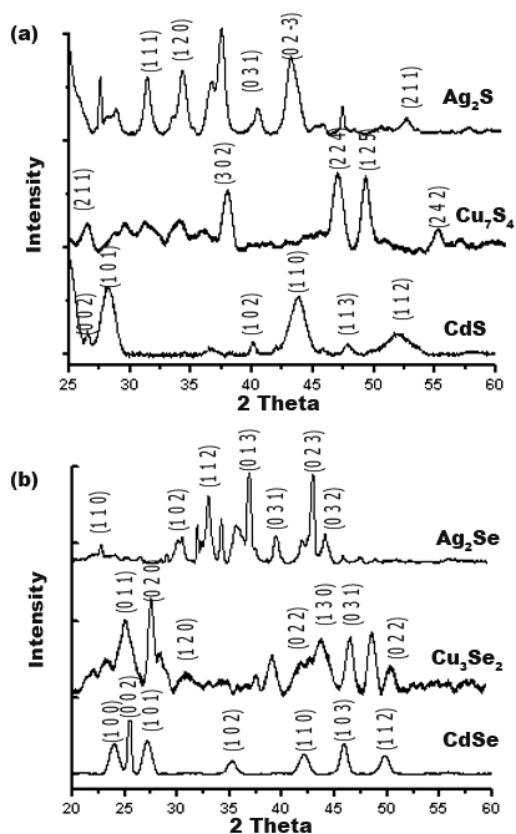


**Fig. 3** XRD data showing (a) CdS,  $\text{Cu}_7\text{S}_4$  and  $\text{Ag}_2\text{S}$  and (b) CdSe,  $\text{Cu}_3\text{Se}_2$  and  $\text{Ag}_2\text{Se}$ .

exchanged resulting in altered stoichiometries and crystal lattices. The hexagonal wurzite CdS nanorods were converted to monoclinic  $\text{Ag}_2\text{S}$  indexed to acanthite (JCPDS 14-0072) and orthorhombic  $\text{Cu}_7\text{S}_4$  indexed to anilite (JCPDS 33-489) respectively. Whereas, CdSe in the wurzite form was converted to orthorhombic  $\text{Ag}_2\text{Se}$  (naumannite JCPDS 71-2410) and tetragonal  $\text{Cu}_3\text{Se}_2$  (umangite JCPDS 47-1745) respectively. Reitveld analysis was also undertaken to ensure that the stoichiometry of the products is correct and can be seen in Table S1&S2 (ESI<sup>†</sup>).

Representative SEM images of the multi-layer assemblies attained using different protocols are shown in Fig. 4. The original CdS multilayer nanorod assemblies can be seen in Fig. S3. The top down image of  $\text{Cu}_7\text{S}_4$  in Fig. 4(a) shows that the dense nanorod assemblies are maintained after cation exchange. Some crack propagation occurs from solvent evaporation although both the close packed order and underlying vertical orientation are clearly evident. The higher resolution SEM image inset more clearly shows the retention of hexagonal close packing in the nanorods after exchange, with an inter rod repeat difference of less than 3nm. A cross section SEM image of an  $\text{Ag}_2\text{Se}$  multilayer nanorod assembly after cation exchange is shown in Fig. 4(b). The assembly initially formed by electrophoretic deposition of  $7 \times 29$  nm CdSe rods, extends over 30 layers with the cation exchange resolute throughout the film thickness. A cross section analysis by EDX was undertaken on the  $\text{Ag}_2\text{Se}$  sample to ensure the spin exchange process is valid to a 30 layer nanorod depth and can be seen in Fig. S4 (e) (ESI<sup>†</sup>).

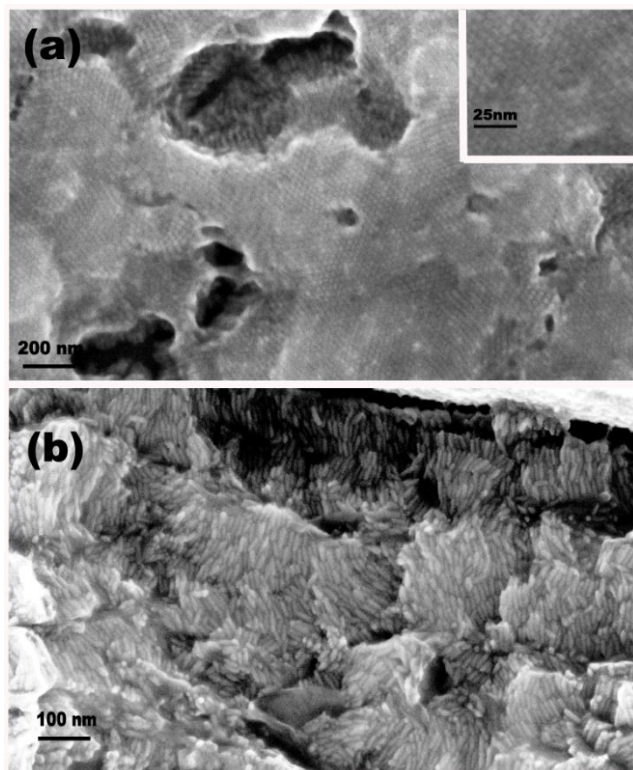


**Fig.4** SEM images of (a) Cu<sub>7</sub>S<sub>4</sub> multilayer nanorod assembly spin exchanged from CdS and inset showing clearly showing tips of nanorods (b) Cross section of Ag<sub>2</sub>Se multilayer nanorod assembly

In order to investigate the surface species and surface composition of CdSe nanorods and the hybrids of cation exchanged Ag<sub>2</sub>Se and Cu<sub>3</sub>Se<sub>2</sub> nanorods, X-ray photoelectron spectroscopy (XPS) analysis was performed. In the case of CdSe, high resolution photoelectron spectrum of Cd 3d was fitted with doublet peaks, with Cd 3d<sub>5/2</sub> appearing at a binding energy of

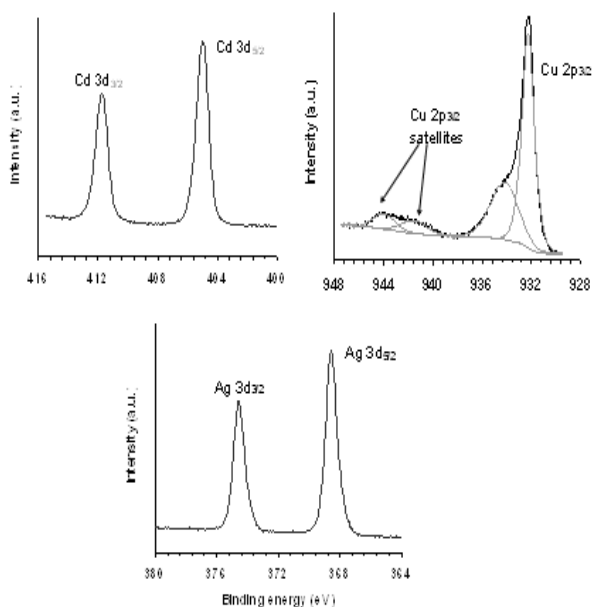


**Fig.5** XPS photoelectron spectra of (a) Cd 3d (b) Cu 2p<sub>3/2</sub> and (c) Ag 3d peaks in the cadmium, copper and silver selenides respectively.

composition ratio of 1.2, and P 2p at 133.2 eV corresponding to P-O present in the phosphonic ligands<sup>16, 17</sup>, the chemistry of synthesized CdSe nanorods was established. Survey spectra of the cation exchanged nanorods showed presence of cadmium in very low concentration (~0.16 atomic %) in the copper selenide nanorods and no cadmium was detected in the silver selenide rods thus highlighting completion of the cation exchange process. High resolution spectra of Ag 3d<sub>5/2</sub> in silver hybrids appear at 368.6 eV<sup>16</sup> and associated selenium as selenide confirms the formation of silver selenide. In the Cu 2p<sub>3/2</sub> spectrum Fig 5b, the main peak appears at a binding energy of 932.3 eV and Se 3d appears at 53.7 eV, both characteristic of copper selenide<sup>16</sup>. The shoulder at 932.3 eV on the principle Cu 2p<sub>3/2</sub> peak indicates oxidation of copper with the shake-up satellite peaks at higher binding energies characteristic of Cu in d<sup>9</sup> configuration ie Cu<sup>+2</sup> state.<sup>16</sup> Ratios obtained for Cu/Se and Ag/Se are higher than for Cd/Se reflecting the different stoichiometries obtained.

A careful approach was required to make electrical contacts for transport studies through the multilayer assemblies. Droplets of In-Ga eutectic were used in a van der Pauw geometry<sup>18</sup> to factor in sheet and contact resistances to the spun cast layers deposited on Schottky metal contacts. This avoids electrical shorting since the droplet is placed on the spun cast layers without wetting the surface or being incorporated between the rods and cracks in the assemblies. Two terminal transport measurements of the In-Ga/assembly/metal junctions were acquired between the substrate metal and the In-Ga ohmic contact and were stable in air allowing reproducible transport measurements between  $\pm 2$ –3 V. Fig. 6(a) summarises the I-V curves from the CdS and its respective cation exchanged Ag<sub>2</sub>S assemblies investigated. Both curves behave as n-type semiconductors.

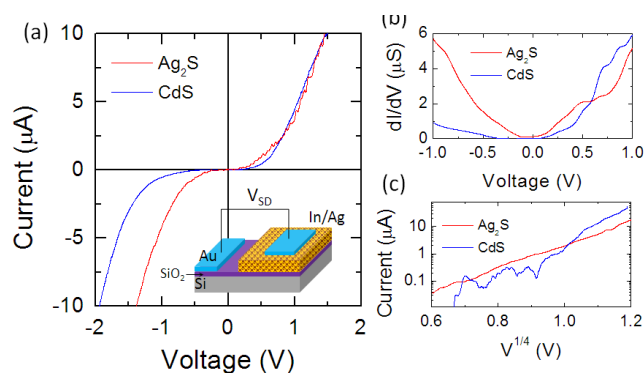


**Fig.6** (a) Current-voltage curves for CdS and Ag<sub>2</sub>S nanorod assemblies with ohmic In-Ga and Schottky Au contacts. (b) differential conductance ( $dI/dV$ ) plots for both assemblies and (c)  $\ln(I)$  vs.  $V^{1/4}$  plots plotted in the potential range greater than respective barrier potential.

As deposited CdS assemblies exhibit some rectification and the positive bias current increasing is exponentially with voltage. The differential conductance ( $dI/dV$ ) in Fig. 6(b) shows an asymmetry consistent with a Schottky barrier limited conduction (see ESI<sup>†</sup>) with weak rectification. When cation exchanged to form Ag<sub>2</sub>S, the I-V response becomes more symmetrical. Analysis of the response (SI ESI<sup>†</sup>) shows that at potentials greater than the barrier height for the material,  $\ln(I)$  scales linearly with  $V^{1/4}$ , as shown in Fig. 6(c). This linearity demonstrates the validity of the thermionic emission model for

the symmetric Ag<sub>2</sub>S multilayer nanorod assemblies, seen more clearly in the symmetric differential conductance plot in Fig. 6c, defined by a gap around zero bias, with sharp conductance onsets at both sides, which is not the case for CdS. In addition, electrical measurements of sintered, thin deposits of the Ag<sub>2</sub>S (ESI†) with very large area contacts show an ohmic response indicative of a highly doped n-type material, with interparticle organic species and gaps which are removed and reduced, respectively. An examination of many of the other proposed mechanisms for transport in these multilayer assemblies, including variable range hopping space-charge-limited, Fowler-Nordheim tunneling, or single electron tunnelling<sup>19</sup> does not describe the data as accurately as the standard Schottky model for CdS and the thermionic emission model for cation exchanged Ag<sub>2</sub>S, which is important considering that in photovoltaic applications, the voltage control over the space charge region, photo-induced carrier generation, separation and extraction depend strongly on carrier transport through the assembly.

The CdS assemblies were also fully exchanged to Cu<sub>7</sub>S<sub>4</sub>, as outlined earlier. Fig. S6(ESI†) shows the resulting I-V curves, and compared to cation exchanged Ag<sub>2</sub>S, the Cu<sub>7</sub>S<sub>4</sub> deposits exhibit a rectifying response similar to CdS assemblies, with a notable difference in that the polarity of the rectification is reversed while keeping the polarity of the applied potential identical. This confirms a change in conduction from being predominantly n-type to that of a p-type assembly since the Cu<sub>7</sub>S<sub>4</sub> now has a Schottky barrier with respect to the In-Ga metal. In both CdS and Cu<sub>7</sub>S<sub>4</sub> assemblies, the reverse bias leakage currents are quite small. Typically, for type-II heterojunctions, rectification is beneficial allowing a voltage controlled depletion or space charge region to form that controls carrier extraction in a solar cell for example. Cu<sub>2</sub>S is typically a highly doped n-type semiconductor and typically forms only ohmic contacts with metals.<sup>20</sup> Estimates of doping densities in the assemblies from thermionic emission theory (see ESI†) shows that the CdS and Ag<sub>2</sub>S n-type semiconductors have carrier concentrations of  $5.4 \times 10^{17} \text{ cm}^{-3}$  and  $6.9 \times 10^{17} \text{ cm}^{-3}$  respectively, with p-type Cu<sub>7</sub>S<sub>4</sub> nanorod assemblies having a doping density of  $5.1 \times 10^{17} \text{ cm}^{-3}$ . The n-type assemblies have electron mobilities of  $8.3 \times 10^{-3} \text{ cm}^2 \text{ V}^{-1} \text{ s}^{-1}$  (CdS) and  $9.05 \times 10^{-3} \text{ cm}^2 \text{ V}^{-1} \text{ s}^{-1}$  (Ag<sub>2</sub>S), while the p-type Cu<sub>7</sub>S<sub>4</sub> has a promisingly high hole mobility of  $8.9 \times 10^{-4} \text{ cm}^2 \text{ V}^{-1} \text{ s}^{-1}$ . The formation of Cu<sub>7</sub>S<sub>4</sub> here shows that a p-type semiconductor cation exchanged multilayer can be formed with sufficient rectification to be potentially compatible with CdS (and also their selenides and tellurides) for heterojunction photon-electron conversion as a multilayer ensemble.

In conclusion, we have shown that cation exchange can be used to transform existing multilayer CdS and CdSe nanorod assemblies into their corresponding silver and copper analogues through the use of a simple spin exchange procedure. We have demonstrated that the superlattice assembly remains intact during the spin exchange process. This technique is generally applicable and can be easily extended to other material systems allowing a greater range of device scale nanorod assemblies to be formed.

## Notes and references

*a*Materials and Surface Science Institute *b*Department of Chemical and Environmental Sciences, *c*SFI-Strategic Research Cluster in Solar Energy

Research, *d* Department of Physics, University of Limerick, Limerick, Ireland. \*E-mail: kevin.m.ryan@ul.ie; Tel: +353 61213167

This work was supported by Science Foundation Ireland (SFI) through the Principal Investigator program, Contract No. 06/IN.1/I85 and the Solar Energy Conversion Strategic Research Cluster [07/SRC/B1160]. This work was also conducted under the framework of the INSPIRE project, funded by the Irish Government's Program for Research in Third Level Institutions, Cycle 4, National Development Plan 2007-2013.

Robert R. Gunning is further acknowledged for his discussions on XRD. † Electronic Supplementary Information (ESI) available: Including experimental data, TEM & corresponding ED, further SEM & XRD analysis and data regarding electrical measurements. See DOI: 10.1039/b000000x/

- 1W. U. Huynh, J. J. Dittmer and A. P. Alivisatos, *Science*, 2002, 295, 2425-2427.
- 2K. M. Ryan, A. Mastroianni, K. A. Stancil, H. Liu and A. P. Alivisatos, *Nano Lett.*, 2006, 6, 1479-1482; I. Gur, N. A. Fromer, M. L. Geier and A. P. Alivisatos, *Science*, 2005, 310, 462-465.
- 3S. Ahmed and K. M. Ryan, *Nano Lett.*, 2007, 7, 2480-2485.
- 4S. Ahmed and K. M. Ryan, *Chem. Comm.*, 2009, 6421-6423.
- 5J. L. Baker, A. Widmer-Cooper, M. F. Toney, P. L. Geissler and A. P. Alivisatos, *Nano Lett.*, 2009, 10, 195-201.
- 6D. Baranov, A. Fiore, M. van Huis, C. Giannini, A. Falqui, U. Lafont, H. Zandbergen, M. Zanella, R. Cingolani and L. Manna, *Nano Lett.*, 2010, 10, 743-749.
- 7T. P. Bigioni, X. M. Lin, T. T. Nguyen, E. I. Corwin, T. A. Witten and H. M. Jaeger, *Nat. Mater.*, 2006, 5, 265-270; M. Zanella, R. Gomes, M. Povia, C. Giannini, Y. Zhang, A. Riskin, M. Van Bael, Z. Hens and L. Manna, *J. Adv. Mater.*, 2011, 23, 2205-2209; A. Singh, R. D. Gunning, A. Sanyal and K. M. Ryan, *Chem. Comm.*, 2010, 46, 7193-7195; C. O'Sullivan, S. Ahmed and K. M. Ryan, *J. Mater. Chem.*, 2008, 18, 5218-5222; T. Bala, A. Sanyal, A. Singh, D. Kelly, C. O'Sullivan, F. Laffir and K. M. Ryan, *J. Mat. Chem.*, 2011, 21, 6815-6820.
- 8H. Liu, J. S. Owen and A. P. Alivisatos, *J. Am. Chem. Soc.*, 2006, 129, 305-312; Y. Yin and A. P. Alivisatos, *Nature*, 2005, 437, 664-670.
- 9B. Mehta, S. Gupta, V. Singh, P. Tripathi and D. Varandani, *Nanotechnology*, 2011, 22, 135701; Y. Wu, C. Wadia, W. Ma, B. Sadtler and A. P. Alivisatos, *Nano Lett.*, 2008, 8, 2551-2555; R. Cope and H. Goldsmid, *Br. J. Appl. Phys.*, 1965, 16, 1501.
- 10R. D. Robinson, B. Sadtler, D. O. Demchenko, C. K. Erdonmez, L.-W. Wang and A. P. Alivisatos, *Science*, 2007, 317, 355-358; B. Sadtler, D. O. Demchenko, H. Zheng, S. M. Hughes, M. G. Merkle, U. Dahmen, L.-W. Wang and A. P. Alivisatos, *J. Am. Chem. Soc.*, 2009, 131, 5285-5293.
- 11J. M. Luther, H. M. Zheng, B. Sadtler and A. P. Alivisatos, *J. Am. Chem. Soc.*, 2009, 131, 16851-16857; P. H. C. Camargo, Y. H. Lee, U. Jeong, Z. Q. Zou and Y. N. Xia, *Langmuir*, 2007, 23, 2985-2992; S. E. Wark, C.-H. Hsia and D. H. Son, *J. Am. Chem. Soc.*, 2008, 130, 9550-9555; A. Dorn, P. M. Allen, D. K. Harris and M. G. Bawendi, *Nano Lett.*, 2010.
- 12D. H. Son, S. M. Hughes, Y. Yin and A. Paul Alivisatos, *Science*, 2004, 306, 1009-1012.
- 13H. K. Boparai, M. Joseph and D. M. O'Carroll, *J. Hazard Mater.*, 2010; J. Li, T. Zhang, J. Ge, Y. Yin and W. Zhong, *Angew. Chem. Int. Ed.*, 2009, 48, 1588-1591.
- 14J. B. Rivest, S. L. Swisher, L.-K. Fong, H. Zheng and A. P. Alivisatos, *ACS Nano*, 2011, 5, 3811-3816.
- 15R. G. Pearson, *J. Am. Chem. Soc.*, 1963, 85, 3533-3539.
- 16V. 3.5, NIST-XPS database, 2011.
- 17K. D. Bomben, J. Chastain, J. Moulder, P. Sobol and W. Stickle, Perkin-Elmer Corporation, Physical Electronics Division, 1992.
- 18L. Van der Pauw, *Rep.*, 1958, 13, 1.
- 19A. J. Houtepen, D. Kockmann and D. Vanmaekelbergh, *Nano Lett.*, 2008, 8, 3516-3520; A. A. Talin, F. Léonard, B. Swartzentruber, X. Wang and S. D. Hersee, *Phys. Rev.*, 2008, 101, 76802; H. Steinberg, Y. Lilach, A. Salant, O. Wolf, A. Faust, O. Millo and U. Banin, *Nano Lett.*, 2009, 9, 3671-3675; D. L. Klein, R. Roth, A. K. L. Lim, A. P. Alivisatos and P. L. McEuen, *Nature*, 1997, 389, 699-701.
- 20M. Leon, N. Terao and F. Rueda, *J. Mat. Chem.*, 1984, 19, 113-120.